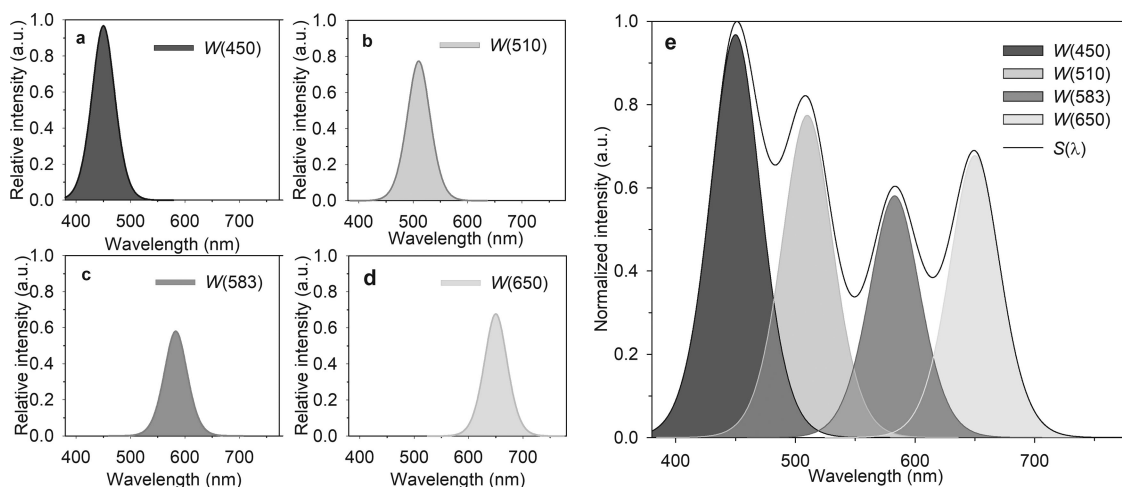


# Illumination in Museums: Four-Primary White LEDs to Optimize the Protective Effect and Color Quality

Volume 11, Number 1, February 2019

Rui Dang  
Nan Wang  
Gang Liu  
Ye Yuan  
Jie Liu  
Huijiao Tan



DOI: 10.1109/JPHOT.2019.2893822

1943-0655 © 2019 IEEE

# Illumination in Museums: Four-Primary White LEDs to Optimize the Protective Effect and Color Quality

Rui Dang , Nan Wang , Gang Liu, Ye Yuan , Jie Liu,  
and Huijiao Tan 

Tianjin Key Laboratory of Architectural Physics and Environmental Technology, School of Architecture, Tianjin University, Tianjin 300072 China

DOI:10.1109/JPHOT.2019.2893822

1943-0655 © 2019 IEEE. Translations and content mining are permitted for academic research only. Personal use is also permitted, but republication/redistribution requires IEEE permission. See [http://www.ieee.org/publications\\_standards/publications/rights/index.html](http://www.ieee.org/publications_standards/publications/rights/index.html) for more information.

Manuscript received January 4, 2019; accepted January 13, 2019. Date of publication January 17, 2019; date of current version February 8, 2019. This work was supported in part by the National Key Research and Development Program under Grant 2018YFC0705103, in part by the Natural Science Fund of Tianjin under Grant 17JCYBJC22400, and in part by the Peiyang Scholar Program under Grant 1801. Corresponding authors: R. Dang and N. Wang (e-mail: dr\_tju@126.com; wangnan94118@126.com).

**Abstract:** Traditional Chinese paintings (TCPs), which are characterized by enormous storage and high value, are prone to suffering from radiation damage from museum illumination, such as color fading, discoloration, and color vanishing, especially for the most light-sensitive traditional Chinese paintings that are painted with organic pigments (op-TCPs). Thus, the development of light sources that minimize the damage to TCPs is essential. Meanwhile, the color quality of light sources is also of great importance, and there is a lack of methodology for obtaining light sources with optimized spectra to simultaneously achieve the protective effect and ensure the color quality. Here, changing curves of the CIE DE2000 color differences of pigments were shown as a function of the exposure duration by calculating the periodically measured color parameters in a long-term illumination experiment under four monochromatic lights. Relative spectral responsivity functions of the op-TCPs were deduced by fitting the experimental data and obtained the corresponding equal-illuminance relative damage formulas. Then, damage laws to the op-TCPs and the lowest color damage spectral power distributions that satisfy the color quality requirements of a four-primary white LED model were obtained. Our results can provide the theory and application basis to manufacture white LEDs that are suitable for illuminating op-TCPs; the method can be further used in preparing white LEDs for other cultural relics.

**Index Terms:** Light-emitting diodes, optimization methods, computer simulation, lighting.

## 1. Introduction

Traditional Chinese paintings (TCPs) represent an important part of the world's cultural heritage, witness the Chinese civilization, and possess extremely high art and cultural value. In addition, many precious paintings have been preserved for generations and contribute to a huge storage of over 640,000 pieces in museums [1].

In total, 50.66% of TCPs preserved in museums of China have suffered irreversible damage to varying degrees [2]. The illumination, temperature, humidity and air quality are damaging factors to TCPs; the latter three can be technically adjusted to the optimal state of preservation, whereas illumination is indispensable because of the visual demand, but all radiation can cause damage

to TCPs [3]. The photochemical material stability of TCPs was identified in high responsivity to illumination in museum exhibits according to the technical report 157: 2004 of the International Commission on de L'Eclairage (CIE) [4] and code for lighting design of the museum of China [5]. Accordingly, the optical radiation of light sources is the main factor that causes severe damage to TCPs, such as color fading, discoloration, and color vanishing [6]. TCPs fall into heavy color paintings painted with inorganic pigments and light color paintings painted with organic pigments. Organic pigments that were produced using juices extracted from the roots, stalks, and leaves of plants are more sensitive to radiation than inorganic pigments, which were mainly made from natural mineral materials [7]. Therefore, we chose the traditional Chinese paintings painted with organic pigments (op-TCPs) as the subject of our study.

The key to protecting TCPs from radiation is the manipulation of the spectral compositions of light sources, where infrared and ultraviolet radiation can seriously damage exhibits [8]; consequently, the elimination of invisible radiation in light sources has achieved a common consensus [9]–[11]. Nonetheless, visible radiation also damages the exhibits and cannot be eliminated because of the required visual effect, so the exploration of the effect of visible radiation appeals to increasingly many researchers [12]–[15]. The results of museum investigations [16] at home and abroad by our research group demonstrate that the most frequently used light sources to illuminate TCPs at present are the halogen lamp, which excludes infrared and ultraviolet radiation, metal halide and white LED. The color damage ratio of these light sources to the TCPs, which is 1.00:0.97:0.91, was acquired by previous research [6] through illumination experiment and analysis of color differences in pigments. The result revealed that white LEDs had a slight advantage in protecting TCPs. Fortunately, SPDs of the white LEDs can be flexibly adjusted according to various needs [17], which forms the basis for further optimizing the spectra and obtaining the desired light sources.

The museum light sources that illuminate TCPs should provide a positive protective effect and pleasurable color quality [18]. Low correlated color temperature ( $CCT \leq 4000$  K) and high color rendering ( $R_a \geq 90$ ,  $R_g > 0$  &  $|Duv| < 0.0054$ ) are the color quality requirements of light sources that illuminate the TCPs in the current standard [5]. For the protective effect, the key to performing the job is obtaining the damage function of the monochromatic lights to the corresponding paintings. The Berlin model [4] was proposed to evaluate the damage extent of visible lights, which was proven to be generally applicable to most materials. However, for the pigments in op-TCPs, the rule may not completely fit. The Berlin model assumes that the damage of the wavelengths behaves with a logarithmic trend. Although we agree on the general rule, to obtain a damage function for op-TCPs, further parameter determination is required based on the Berlin model because the op-TCPs have specificity, including distinctive colors and ingredients compared to foreign materials, based on which the Berlin model parameters were deduced.

At present, the SPDs of white LEDs that satisfy the above prerequisites mostly contain the primaries of red, amber, green, and blue [19]–[22], and these LEDs are called red/amber/green/blue (RAGB) four-primary white LEDs. Currently, the four-primary mixture method [23], [24] is mainly used to develop SPDs of white LEDs based on specific requirements. Thus, it is meaningful and plausible to perform spectral optimization on four-primary white LEDs to minimize the damage effect while maintaining the color quality, so that a new type of white LED can be developed to illuminate op-TCPs.

The differences in the SPDs derive from the variations in intensity distributions of the four monochromatic wavebands. The brute-force method can realize an accurate and complete iteration of the intensities and form various SPDs, which enables further assessment and selection of the spectra.

Here, we conducted a long-term experiment to illuminate specimens of op-TCPs with monochromatic lights in red, amber, green and blue. We periodically tested the color parameters of pigments, calculated the CIE DE2000 color differences [25] after all illumination cycles, plotted the changing curves of the color differences as a function of time and evaluated the degree of damage of the monochromatic lights. Furthermore, we proposed the color damage functions of the op-TCPs by amending the Berlin function. Base on the obtained functions, we used a four-primary white LED as an example to conduct a spectral evaluation and selection to realize the spectral optimization. A

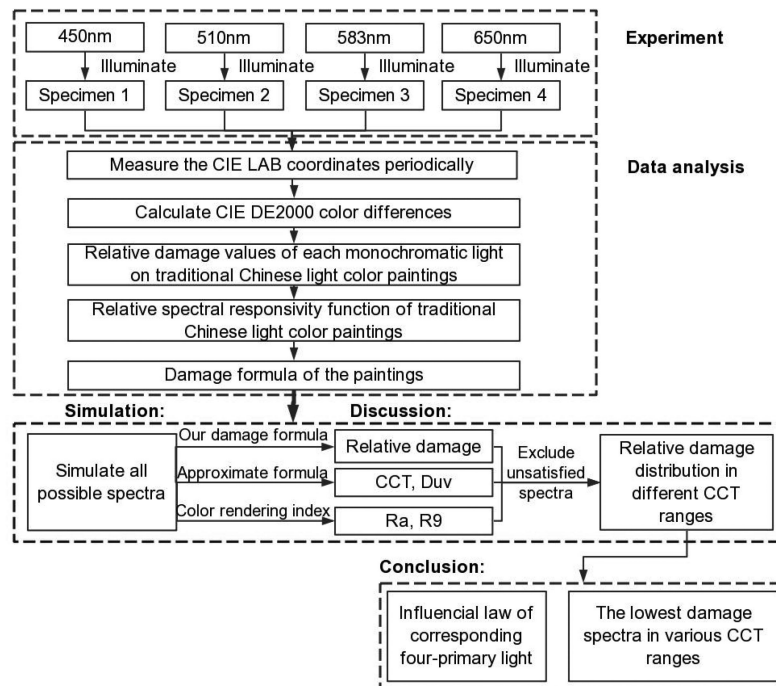


Fig. 1. Research technical roadmap.

peak wavelength optimization of the blue component was conducted to explore the potential lower damage spectra. Finally, we concluded our research value and extended our method. The research technical roadmap is shown in Fig. 1.

## 2. Materials and Methods

### 2.1 Models of Specimens

Four groups of specimens of op-TCPs were crafted by the traditional Chinese Painting Institute of Tianjin University using traditional techniques and materials. First, the most typical organic pigments (indigo (cyan in color), cambogia (yellow), carmine (red), and pine-ink (black)) were dissolved into water with the proportion of 1:1 to certify the same concentration; second, the pigments were evenly sprayed on separate sheets of rice paper and manually framed with wheat starch paste using traditional techniques to imitate the actual op-TCPs; third, four sheets of rice paper painted with organic pigments were cut and recombined to obtain four specimens, each of which contained indigo, cambogia, carmine, and pine-ink, at equal sizes of 2.3 cm by 2.3 cm; finally, three points (0.4 cm x 0.4 cm) were marked on each pigment of all specimens. The color parameters of the points were tested, and the average values were calculated to minimize the measuring errors. One of the four specimens is presented in Fig. 2.

### 2.2 Experimental Light Sources

Four monochromatic light sources with the peak wavelengths of 450 nm, 510 nm, 583 nm, and 650 nm were produced by a museum tungsten halogen lamp (PHILIPS 6423F0) with infrared cut-off filters and 20-nm narrow band-pass filters, which peaked at 450 nm, 510 nm, 583 nm, and 650 nm (Specialized from Institute of Optics, Fine Mechanics and Physics, Chinese Academy of Sciences). To ensure the precision of the experiment, all monochromatic light spectra were detected by a spectroradiometer (HIDAMARI S-2440) to determine their spectral irradiance distribution on

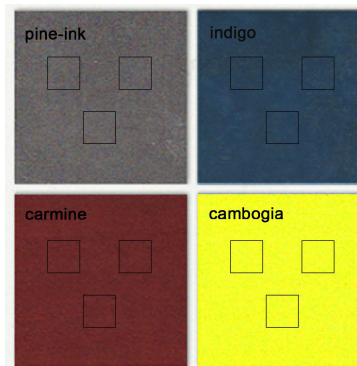


Fig. 2. One of four specimens illuminated by four light sources.

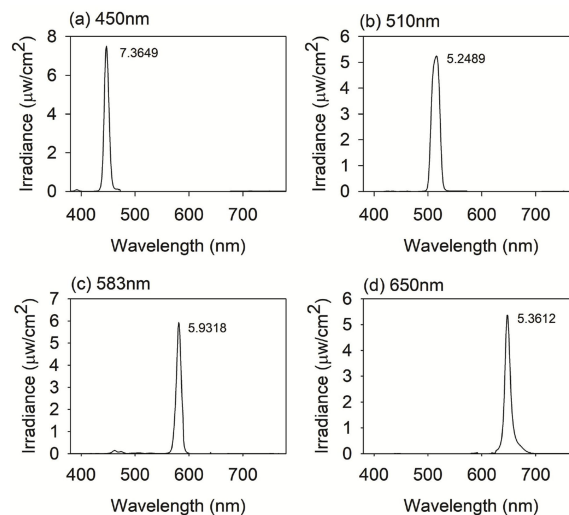


Fig. 3. Irradiance distribution of four monochromatic lights on the surface of the specimens: (a) 450 nm; (b) 510 nm; (c) 583 nm; (d) 650 nm.

the surface of the specimens (Fig. 3). The total irradiance of each light source over the entire waveband was maintained at  $1 \text{ W/m}^2$  during the long-term experiment, and the illuminances of the four monochromatic light sources were 143.68 lx, 400.72 lx, 510.38 lx and 170.57 lx, respectively. We examined the irradiance of the light sources in every test cycle and changed the light source immediately when light fading occurred.

In addition, the color parameters in all cycles were tested under the D65 light source (OSRAM, L30W/965,  $6500 \pm 200 \text{ K}$ ), which was calibrated in the National Institute of Metrology of China to confirm the color measurement.

### 2.3 Experimental Methodology

The experiment was conducted in the Optical Laboratory of Tianjin University, whose physical environment was maintained as required to preserve TCPs in the museum [26]: the entire laboratory had constant values of  $23 \pm 0.5^\circ\text{C}$ , 50% and  $0.5 \text{ d}^{-1}$  for the temperature, relative humidity, and air exchange rate, respectively.

Four monochromatic lights were installed on the upper part of the illumination experimental bench, and four identical specimens were simultaneously put under the corresponding light sources. The irradiance on the surfaces of the four specimens was fixed at  $1 \text{ W/m}^2$  by adjusting the output power

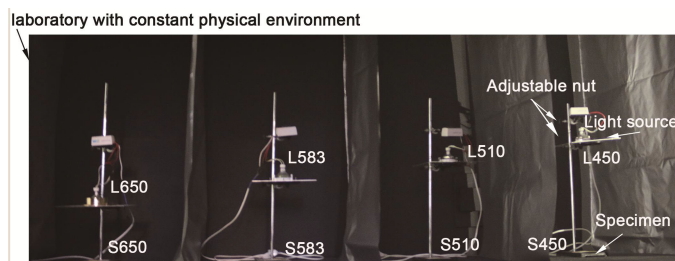


Fig. 4. Experimental device in the optical laboratory; L represents the monochromatic light source; S represents the specimen.

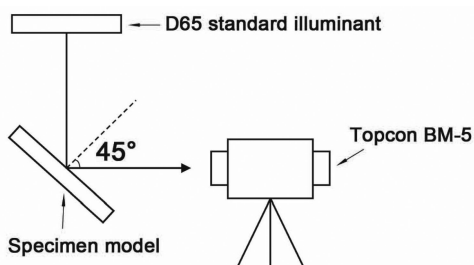


Fig. 5. Diagrammatic sketch of the test environment to measure the color parameters of the pigments painted on the specimens by the Luminance Colorimeter (Topcon BM-5) under the D65 standard illuminant.

and height of the light sources. Four groups were kept independent by shades to avoid mutual interference.

Periodical illumination on specimens was performed. One illumination cycle contained six days with twelve hours per day; the experiment lasted twenty cycles for a total of 1440 hours of illumination. The exposure of the specimens accumulated with the increase in illumination hours. The experimental device is illustrated in Fig. 4.

## 2.4 Test of the Parameters

After each illumination cycle, the specimens were moved under the D65 standard light source; the color parameters of the specimens were measured by the standard color test method of CIE [27] (Fig. 5).

The CIELAB chromaticity coordinates ( $a^*$ ,  $b^*$ ) and metric brightness value  $L^*$  of four specimens were measured before and each cycle after the illumination [28] at the test points marked in Fig. 2 by the Luminance Colorimeter (Topcon BM-5 with an accuracy of  $\pm 3\%$ ). The color parameters of each pigment in each specimen were determined by the average value of the three testing points to minimize the measuring errors. The color differences of the four pigments (indigo, cambogia, carmine, and pine-ink) were calculated using the CIE DE2000 formula [29] by comparing the color of the specimen in each cycle with the initial unirradiated values. The formula of CIE DE2000 is shown as (1):

$$\Delta E_{00}^* = \sqrt{\left(\frac{\Delta L'}{K_L S_L}\right)^2 + \left(\frac{\Delta C'}{K_C S_C}\right)^2 + \left(\frac{\Delta H'}{K_H S_H}\right)^2 + R_T \left(\frac{\Delta C'}{K_C S_C}\right) \left(\frac{\Delta H'}{K_H S_H}\right)} \quad (1)$$

where  $\Delta L'$  is the lightness difference,  $\Delta C'$  is the chroma difference, and  $\Delta H'$  is the hue difference;  $K_L$ ,  $K_C$ , and  $K_H$  are the weighing factors for the lightness, chroma and hue, whose values are  $K_L = K_C = K_H = 1$  here, and can be adjusted for various viewing conditions;  $S_L$ ,  $S_C$ , and  $S_H$  are the

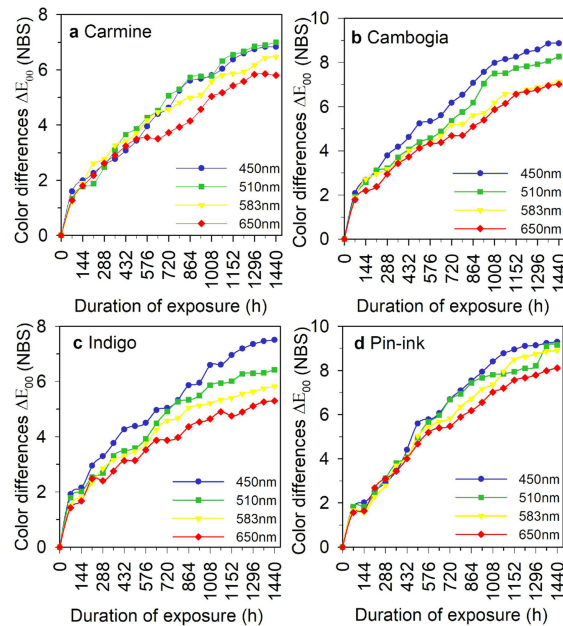


Fig. 6. Changing curve of the CIE DE2000 color differences of the pigments: (a) Carmine; (b) Cambogia; (c) Indigo; and (d) Pine-ink under the illumination of monochromatic lights with peak wavelengths of 450 nm, 510 nm, 583 nm, and 650 nm with an increase in exposure duration.

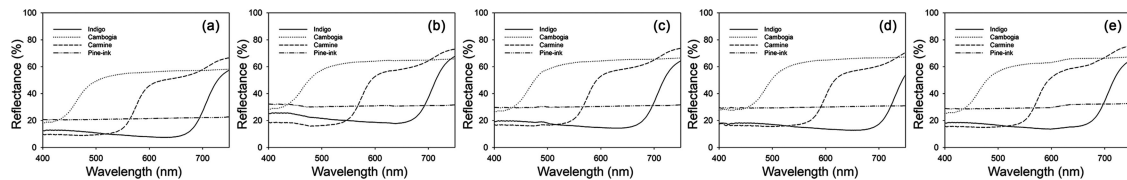


Fig. 7. Spectral reflectance of the pigments (a) unirradiated and after the illumination of monochromatic lights with peak wavelengths of (b) 450 nm, (c) 510 nm, (d) 583 nm, and (e) 650 nm.

compensations for the lightness, chroma, and hue, respectively.  $R_T$  accounts for the rotation of the ellipses in blue.

### 3. Experimental Results

#### 3.1 Changing Curves of Color Differences

The changing laws of color differences  $\Delta E_{00}^*$ , which periodically varied with the accumulation of illumination hours (which is equal to the duration of exposure), are shown in Fig. 6. The color differences in the pigments increased with increasing exposure, which indicates that the illumination increasingly affects the color change of the pigments, and monochromatic lights with different wavelengths contribute differently to the color change of the same pigment.

The spectral reflectances of the pigments before and after the illumination of the four monochromatic lights are shown in Fig. 7.

#### 3.2 Relative Damage Values of Monochromatic Lights

The damage of a monochromatic light to one pigment is determined by the average values over twenty cycles, whose time duration is 1440 hours. Thus, for one pigment influenced by a light source,

TABLE 1  
Relative Damage Values of Monochromatic Lights to Pigments

	450 nm	510 nm	583 nm	650 nm
<b>Carmin</b>	0.83	0.85	0.80	0.71
<b>Cambogia</b>	1.10	1.00	0.90	0.85
<b>Indigo</b>	0.93	0.82	0.76	0.68
<b>Pine-ink</b>	1.14	1.08	1.05	0.98
<b>Average</b>	1.00	0.94	0.88	0.81



Fig. 8. Examples of the (a) realistic light color painting, (b) small turquoise light color painting, and (c) ink light color painting.

TABLE 2  
Relative Damage Values of Monochromatic Lights on Pigments

	450 nm	510 nm	583 nm	650 nm
<b>Realistic</b>	1.00	0.94	0.88	0.81
<b>Small turquoise</b>	1.03	0.95	0.90	0.83
<b>Ink</b>	1.14	1.08	1.05	0.98

the color difference can be described as  $\overline{\Delta E_{00}^*} = \frac{1}{20}(\Delta E_{00,1}^* + \Delta E_{00,2}^* + \dots + \Delta E_{00,20}^*)$ . To evaluate the relative damage of different monochromatic lights to the pigments, the average damage of the 450-nm monochromatic light to the four pigments is defined as 1.00, to which other values are normalized. The average damage of the light sources to the four organic pigments (indigo, cambogia, carmine, and pine-ink) is shown in Table 1.

The op-TCPs are classified as realistic light color paintings, small turquoise light color paintings, and ink light color paintings, as Fig. 8 shows. Among them, realistic light color paintings are painted with indigo, cambogia, carmine, and pine-ink. We assume that the damage of monochromatic lights to realistic light color paintings can be represented by the average damage to indigo, cambogia, carmine, and pine-ink. Thus, the ratio is  $K_1(450): K_1(510): K_1(583): K_1(650) = 1.00: 0.94: 0.88: 0.81$ , as shown in Table 2. Similarly, small turquoise light color paintings consist of indigo and pine-ink; the ratio of damage of the four monochromatic lights to them is  $K_2(450): K_2(510): K_2(583):$



$K_2(650) = 0.88: 0.95: 0.90: 0.83$ . For the ink light color paintings, which are made of pine-ink, the ratio is  $K_3(450): K_3(510): K_3(583): K_3(650) = 1.14: 1.08: 1.05: 0.98$ .

#### 4. Damage Formula of Four-Primary WLEDs to op-TCPs

The guideline in CIE 157: 2004 [4] determines the level of damage of the light sources to the exposed objects as (2):

$$D = \int_{380}^{780} \Phi(\lambda) \cdot S(\lambda) \cdot t \quad (2)$$

where  $D$  is the relative optical damage flux;  $\Phi$  is the power of incident radiation;  $S$  is the relative spectral responsivity of the materials to the corresponding wavelength  $\lambda$  of the incident radiation; and  $t$  is the duration of exposure.

Thus, the damage degree to the exposed object is determined by the power of incident light, relative spectral responsivity of the materials to the incident radiation, and illumination hours.

The relative spectral responsivity of the materials to the incident radiation is expressed by the Berlin model. The Berlin model is an exponential function deduced by Berlin researchers by exposing representative materials in museums under selected spectral bands; the relative spectral responsivity function is shown as (3). For different materials, various  $b$  values were determined by the researchers. However, op-TCPs are not among the investigated materials. In fact, because of the distinctive color and ingredient of the paintings, the values of  $a$  and  $b$  that we derived from our data are peculiar.

$$S(\lambda) = ae^{-b\lambda} \quad (3)$$

Four monochromatic lights were selected in our experiment to determine  $a$  and  $b$ . The peak wavelengths of the selected monochromatic lights were 450 nm, 510 nm, 583 nm, and 650 nm. Thus, the corresponding damage ratio to the paintings should be theoretically expressed as (4).

$$\begin{aligned} D(450) : D(510) : D(583) : D(650) = \\ \Phi(450) \cdot S(450) \cdot t(450) : \Phi(510) \cdot S(510) \cdot t(510) : \\ \Phi(583) \cdot S(583) \cdot t(583) : \Phi(650) \cdot S(650) \cdot t(650) \end{aligned} \quad (4)$$

The irradiance of four monochromatic lights on the specimens was fixed at an identical value in the experiment, i.e.,  $\Phi(450) = \Phi(510) = \Phi(583) = \Phi(650)$ ; meanwhile, the illumination hours of each group were identical:  $t(450) = t(510) = t(583) = t(650)$ . Therefore, the ratio of  $D$  is theoretically equal to that of  $S$ , which is shown as (5):

$$\begin{aligned} D(450) : D(510) : D(583) : D(650) = \\ S(450) : S(510) : S(583) : S(650) \end{aligned} \quad (5)$$

According to the experiment result, taking the realistic light color paintings as an example, the damage ratio of the four monochromatic lights is  $D_1(450): D_1(510): D_1(583): D_1(650) = K_1(450): K_1(510): K_1(583): K_1(650) = 1.00: 0.94: 0.88: 0.81$ . Thus:

$$\begin{aligned} S(450) : S(510) : S(583) : S(650) = D(450) : D(510) : \\ D(583) : D(650) = 1.00 : 0.94 : 0.88 : 0.81 \end{aligned} \quad (6)$$

(5) implies that the only factor that causes the color damage in our experiment is the relative spectral responsivity of the materials to the incident radiation. Thus, through the experiment, we can obtain the relative spectral responsivity of the TCPs to the four monochromatic lights. When the illumination hours and power of the incident lights are identical, the relative spectral responsivity of the realistic light color paintings to the four monochromatic lights is 1.00: 0.94: 0.88: 0.81. Similarly, the ratios of the small turquoise light color paintings and ink light color paintings are 1.03: 0.95: 0.90: 0.83 and 1.14: 1.08: 1.05: 0.98, respectively.

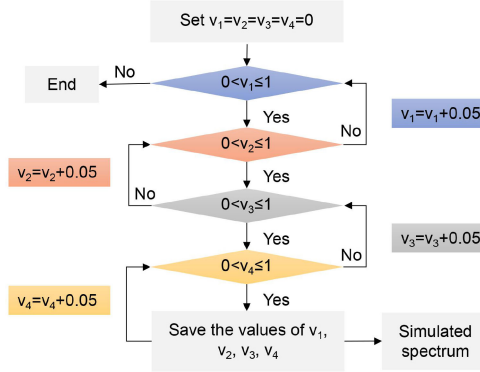


Fig. 9. Iteration flow chart.

For realistic light color paintings, using the proportional values of 1.00, 0.94, 0.88, and 0.81 as representative damage values of 450 nm, 510 nm, 583 nm, and 650 nm to fit the Berlin model using exponential fitting, the corresponding relative spectral responsivity function is  $S_1(\lambda) = 1.593e^{-0.001032\lambda}$  with an R-square value of 0.9962; Similarly, the functions are  $S_2(\lambda) = 1.637e^{-0.001042\lambda}$  for the small turquoise light color paintings with an R-square value of 0.9881 and  $S_3(\lambda) = 1.566e^{-0.0007104\lambda}$  for the ink light color paintings with an R-square value of 0.9714.

After we have obtained the relative spectral responsivity functions of the paintings, the relative damage formula of the op-TCPs under light sources is available, as (2) demonstrates. For different painting types, different relative spectral responsivity functions are put into (2). The illumination hour  $t$  is deleted from the function because  $t$  is identical for the compared light sources.

To compare the damage extent of different light sources, the unequal energy influence should be avoided. In realistic commercial use of the spectral evaluation, the illuminance is generally concerned; thus, an equal-illuminance relative damage formula is deduced:

$$D_L = \int_{380}^{780} \Phi(\lambda) \cdot S(\lambda) \cdot d\lambda \bigg/ \int_{380}^{780} \Phi(\lambda) \cdot V(\lambda) \cdot d\lambda \quad (7)$$

where  $S(\lambda)$  has three options:  $S_1(\lambda) = 1.425e^{-0.001226\lambda}$  for the realistic light color paintings;  $S_2(\lambda) = 1.637e^{-0.001042\lambda}$  for the small turquoise light color paintings; and  $S_3(\lambda) = 1.248e^{-0.001083\lambda}$  for the ink light color paintings.

## 5. Spectral Optimization

A four-primary white LED model with peak wavelengths of 450 nm, 510 nm, 583 nm, and 650 nm and a full width at half maximum (FWHM) of 50 nm [30] was chosen as an example to perform the optimization procedure. The specific peak wavelengths and FWHMs were selected because of the easier acquisition of color quality satisfied spectra [31]. The SPD of the four-primary LED can be considered an outcome weighted by the intensity factors and spectra of the four monochromatic lights. To further iterate the spectral intensities of the four monochromatic lights using the brute-force method, the selected spectrum was first divided into four normalized monochromatic spectra through peak separation. In the iteration process, the relative intensity coefficients  $V_1 - V_4$  were multiplied by the monochromatic wavebands.  $V_1 - V_4$  can achieve the values of 0-1 with intervals of 0.05. Each time  $V_1 - V_4$  were iterated (the iteration flow chart is shown in Fig. 9), a new SPD, which was the basis for calculating all evaluation parameters, was developed by superimposing the monochromatic lights with the new intensities according to the principle of additive spectrum mixture [32], [33], as shown in Fig. 10. Using the brute-force method [34], 194481 pieces of SPDs were developed in total.

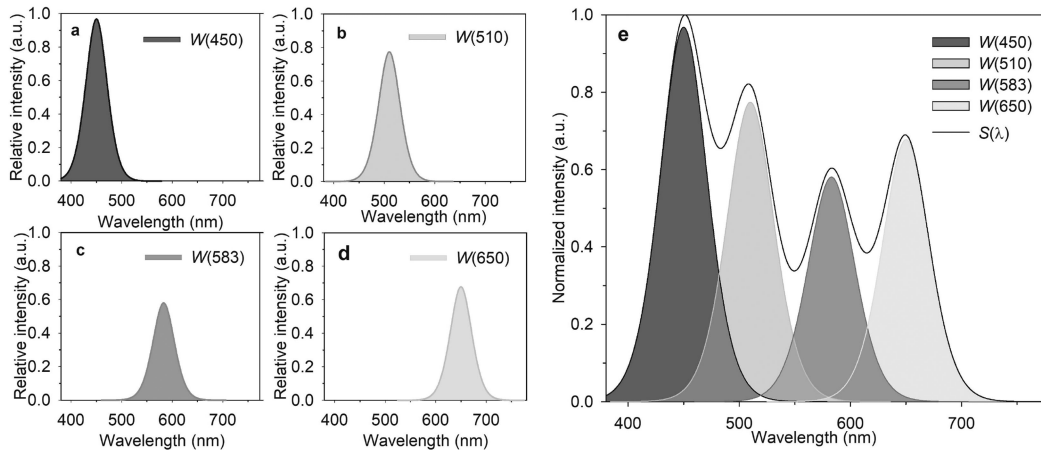


Fig. 10. Spectrum of monochromatic lights with peak wavelengths of (a) 450 nm, (b) 510 nm, (c) 583 nm, and (d) 650 nm;  $w$  is the spectral power of the light; (e) spectral diagram of the RAGB four-primary WLED obtained by the accumulation of the monochromatic lights, where  $S$  is the SPD of the WLED.

The general color rendering index  $R_a$  and special color rendering index  $R_9$  of the obtained 194481 SPDs were calculated using the color rendering index (CRI), which is the most widely used method to evaluate the color quality [35]. The distance from the Planckian locus ( $D_{uv}$ ) of the obtained SPDs was calculated by the simplified appropriate formula [36]. The color rendering requirements [6] for the light sources that illuminated the op-TCPs, which were  $R_a \geq 90$ ,  $R_9 > 0$ , and  $|D_{uv}| < 0.0054$ , were taken as the guideline to remove the dissatisfied SPDs. Then, 4686 pieces remained.

Afterwards, the CCTs of the remaining 4686 SPDs were calculated by McCamy's approximate formula [37]. The guideline of  $2700 \text{ K} \leq \text{CCT} \leq 4000 \text{ K}$  was used to further exclude the dissatisfied SPDs, after which 921 pieces remained.

These 921 SPDs satisfied all required figures of merit related to the color quality in museum illumination. Then, we calculated the equal-illuminance relative damage values  $D_L(\lambda)_1 - D_L(\lambda)_{921}$  of the 921 SPDs to realistic light color paintings, small turquoise light color paintings, and ink light color paintings. The relationships between  $D_L(\lambda)$  and CCTs, the amount of satisfied SPDs and CCT ranges, and the relative average damage values and CCT ranges (the CCT ranges are at intervals of 100, e.g., 2650–2750 K represents the range of 2700 K) are shown in Fig. 11.

From the results of the equal-illuminance relative damage values, we deduced some basic damage laws pertaining to the op-TCPs that suffered from the corresponding four-primary light sources, as shown in Fig. 11:

1. As Fig. 11(a-c) indicate, the relationships between the relative damage of the light sources and the CCTs are identical for the realistic light color paintings, small turquoise light color paintings and ink light color paintings. Hence, the proportional discrepancies of the relative spectral responsivity function among the three types of paintings are too minor to cause apparent differences that can change the relative relationship between the CCTs and the relative damage values. Thus, when one uses the optimization method in the application, it is feasible to use any of the three functions to represent the property of the op-TCPs, as the simulation result illustrates. The reduction of the function amount makes the method easier to apply, so we recommend using one function to form the relative damage formula of the op-TCPs, as (8) represents:

$$D_L = \int_{380}^{780} \Phi(\lambda) \cdot e^{-0.001083\lambda} \cdot d\lambda / \int_{380}^{780} \Phi(\lambda) \cdot V(\lambda) \cdot d\lambda \quad (8)$$

2. Although the relative damage distributions are similar among the three types of paintings, the absolute values of damage for the paintings vary. The amount of difference does not work on

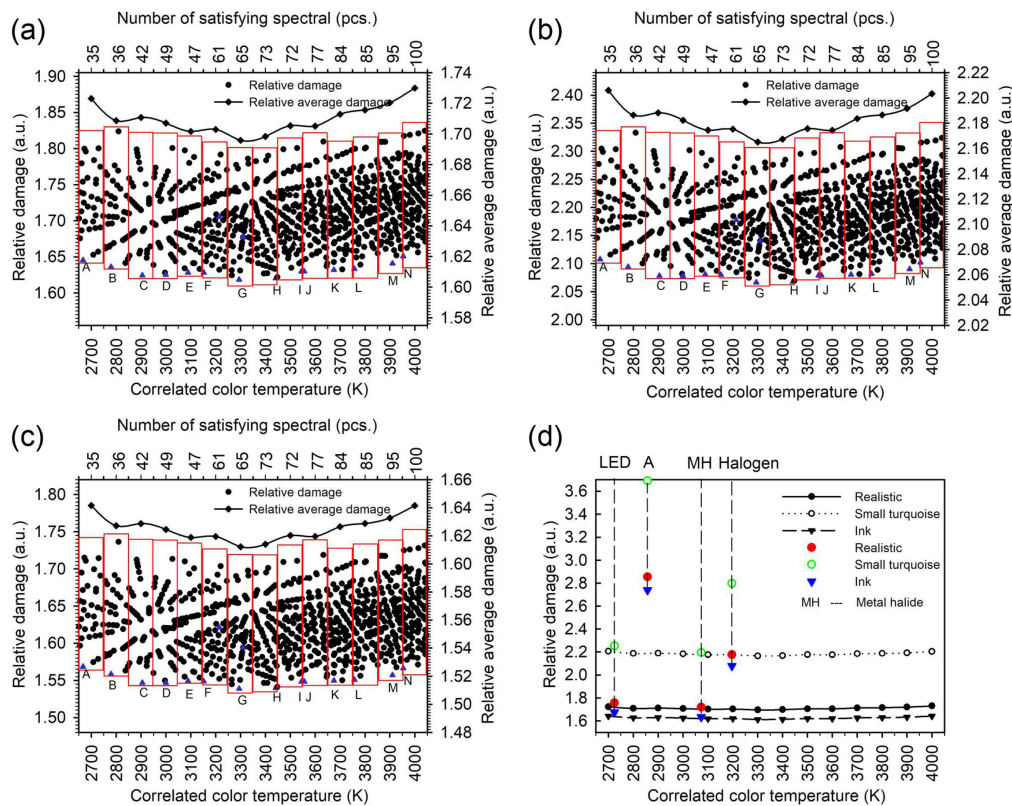


Fig. 11. Diagram of the  $D_L(\lambda)$  values, amount of satisfied SPDs and relative average damage to (a) realistic light color paintings, (b) small turquoise light color paintings, and (c) ink light color paintings in different ranges of CCT. The points of SPD with the same CCT range are enclosed by the red rectangle. (d) Relationship between the lowest damage spectra in all CCT ranges and the metal halide light, off-the-shelf LED, standard A illuminant and halogen lamp.

the light source evaluation and selection, but it indicates that when illuminated by the same light source, the small turquoise light color paintings suffer the most serious color change, and the ink light color paintings sustain the least damage.

- In general, the relative average damage values first display a decreasing trend at 2700–3300 K, after which they increased. Thus, through our experiment and simulation, it was discovered that 3300 K is the most desirable CCT in museum illumination.
- The number of SPDs that satisfy the color rendering requirements increases with the increase in CCTs (the upper axis of Fig. 11) except for two minor decreases at 3100 K and 3500 K, e.g., the number of qualified SPDs is 35 and 100 in the ranges of 2700 K and 4000 K.
- When producing white LEDs, to protect cultural relics, the SPD with the lowest relative damage value should be preferentially selected, i.e., SPD G in the range of 3300 K is preferable. However, if SPD G cannot be manufactured because of technical restrictions, other points can be developed with the damaging order from low to high.
- If light sources with specific CCTs are required for reasons such as exhibition effects, the selection begins with the lowest damage point in the corresponding CCT region.
- Each point represents one SPD. There are 921 pieces in total, which are too many to completely display in the paper. Therefore, we show the SPDs with the lowest relative equal-illuminance damage in the entire CCT range [SPDs of points A-N in Fig. 11(a, b, c)]. Points A-N are the same in Fig. 11(a, b, c) according to the simulation results. The relative damage values  $D_L$ , color rendering index  $R_a$  and  $R_9$ , and distance  $D_{uv}$  from the Planckian locus of the lowest damage SPDs are listed in Table 3.

TABLE 3  
 Figures of Merit of the Lowest Damage SPDs in 2700–4000 K

CCT Range	CCT	$D_{L1}$	$D_{L2}$	$D_{L3}$	$R_a$	$R_9$	Duv
2700 (A)	2667	1.6453	2.1075	1.5681	91.32	80.54	0.00470
2800 (B)	2779	1.6359	2.0939	1.5583	90.97	76.76	0.00416
2900 (C)	2905	1.6242	2.0780	1.5466	91.07	76.70	0.00525
3000 (D)	2999	1.6250	2.0778	1.5467	90.90	74.07	0.00438
3100 (E)	3089	1.6280	2.0806	1.5489	90.98	73.51	0.00393
3200 (F)	3152	1.6281	2.0800	1.5486	90.73	71.22	0.00347
3300 (G)	3294	1.6183	2.0665	1.5387	90.53	68.87	0.00477
3400 (H)	3442	1.6203	2.0677	1.5398	90.35	66.26	0.00475
3500 (I)	3544	1.6295	2.0786	1.5481	90.61	67.02	0.00442
3600 (J)	3556	1.6297	2.0789	1.5483	90.82	68.59	0.00489
3700 (K)	3675	1.6318	2.0804	1.5496	90.20	63.00	0.00421
3800 (L)	3757	1.6332	2.0817	1.5507	90.48	64.68	0.00525
3900 (M)	3910	1.6406	2.0899	1.5570	90.15	61.00	0.00484
4000 (N)	3954	1.6506	2.1022	1.5662	90.04	59.60	0.00346

<sup>a</sup> $D_{L1}$ ,  $D_{L2}$ , and  $D_{L3}$  represent the relative damage values of the realistic light color paintings, small turquoise light color paintings, and ink light color paintings, respectively.

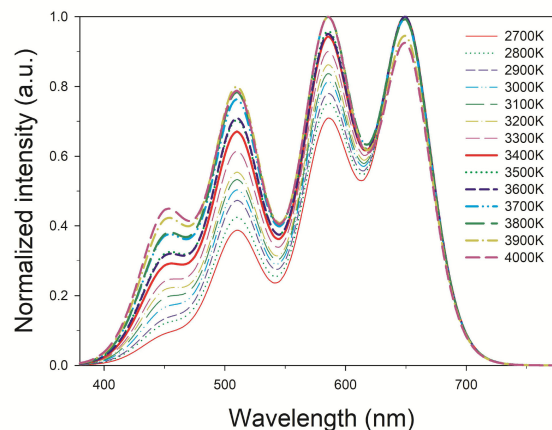


Fig. 12. Lowest damage SPDs that satisfy the requirements of color rendering in the range of 2700–4000 K.

The lowest damage SPDs in the range of 2700–4000 K were fitted according to spectral intensities  $V_1 - V_4$ , as shown in Fig. 12. The SPDs in Fig. 12 are the ideal SPDs in different CCT ranges, which should be chosen first in realistic production. The acquisition of the visually satisfying lowest damage SPDs realizes the spectral optimization of the four-primary white LED.

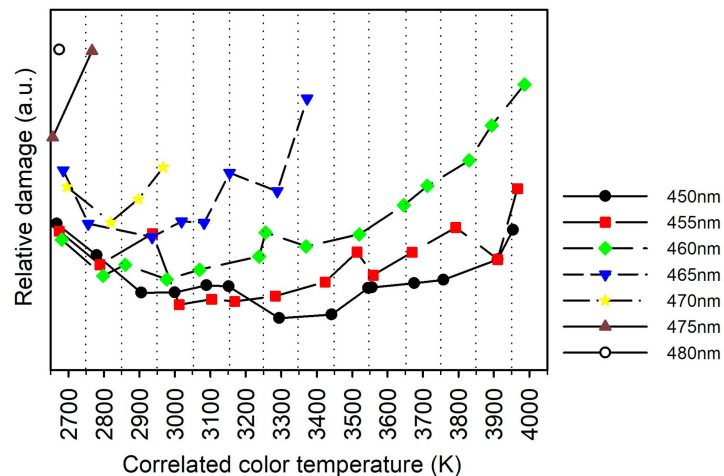


Fig. 13. Lowest relative damage values of the spectra with various peak wavelengths of the blue component in different CCTs.

The relative equal-illuminance damage values of the halogen light, metal halide light, off-the-shelf LED, and standard A illuminant were calculated and compared with the lowest damage spectra in the optimized system. Fig. 10(d) shows that the optimized system performs better than the current light sources in op-TCP protection. However, the advantage of the lowest damage spectra to the calculated metal halide light, which is in the 3100 K range, is limited, so lower damage spectra can be achieved by adjusting the peak wavelengths. Thus, the spectral optimization can be used to find the lowest damage spectra for specific LED components and perform peak wavelength optimization to find better spectra. In application, the peak wavelength optimization can guide the component substitution for further optimization. Here, because the blue region plays the most important role in the color damage, a peak wavelength optimization for the blue component (currently 450 nm) was conducted to lower the damage.

Apart from the iteration of  $V_1$ – $V_4$ , the peak wavelength of the blue component was iterated from 450 nm to 485 nm with a step of 5 nm. Although the FWHM of the component changes with the change in peak wavelength because of the restriction of the preparation technology of the component, we assume that the FWHM remains at 50 nm in our optimization. In practice, the FWHM of the realistic LED chip that the manufacturer achieved should be substituted in the optimization. All color quality satisfied spectra were evaluated by (8).

As Fig. 13 demonstrates, using the 455-nm blue component instead of the 450-nm one reduces the lowest damage extent in the 3100 K CCT range. However, the result is not consistent with our imagination. In theory, the usage of the blue components with longer wavelengths, to which the pigments are less sensitive, will decrease the damage. However, Fig. 13 shows that in most CCT ranges, the 450-nm component realizes the lowest damage because the optimization simultaneously considers the effect of the damage extent and color quality. Although the blue components with longer wavelengths damage the op-TCPs less, the advantage disappears after considering the color quality requirements. Thus, in the selection of LED components, it is unreasonable to only pick longer wavelengths without considering their properties of color quality.

## 6. Conclusion

The irradiances of light sources obviously affect the color change of the op-TCPs. The influence law is illustrated in Fig. 6; the relative spectral responsivity functions of the realistic light color paintings, small turquoise light color paintings and ink light color paintings are demonstrated. Through our simulation, we conclude that the effect of the relative spectral responsivity of the three types of op-TCPs is minor considering the slight discrepancy of the proportions. Thus, we recommend using

one formula instead of three to express the damage extent. The equal-illuminance damage formula of white LEDs to the op-TCPs is shown in (8).

When satisfying the color-rendering requirements ( $R_a \geq 90$ ,  $R_g > 0$  &  $|Duv| < 0.0054$ ), the “correlated color temperatures (CCTs),” “spectra amount in different ranges of CCTs,” and “relative equal-illuminance damage of each spectrum to the op-TCPs” of the optimized four-primary white LEDs have clear relationships, as demonstrated in Fig. 10. Some basic laws of the damage to the op-TCPs are discovered, and practical suggestions about our achievements are provided.

The method can be used to support the development of a new type of white LED to illuminate op-TCPs. The achievement also offers white LEDs with the favorable spectra with 450 nm, 510 nm, 583 nm and 650 nm in CCTs at 2700–4000 K according to the consideration of relative equal-illuminance damage. In practice, the production of this new type of white LED with spectra that cause the least damage should be first selected, as shown in Fig. 11.

When we select the LED components to perform the optimization, it is unreasonable to directly select those with longer wavelengths considering the damage effect. The peak wavelength optimization should be conducted first to obtain the optimizing components. Although the extensive application of the peak wavelength optimization in reality still has a long way to go because of the restriction of the current LED manufacturing level, the method can offer guidance for LED component designers.

The method flow of the illumination experiment, data analysis, and optimization of the spectra can be extended to develop spectra of white LEDs for other high-responsivity cultural relics such as lacquerwares, frescos, folding screens, and dyed silks. In addition, the white LED spectra that we obtained using the method flow are applicable for different types of cultural relics and can be manufactured because of the tunable characteristics of white LEDs, which can fundamentally solve the problem of protective illumination of cultural relics.

## References

- [1] “The Thirteenth Five” Plan of National Heritage Development, State Administration of Cultural Heritage in People’s Republic of China, 2017.
- [2] L. Chen, “Research on the development strategy of museum in “Internet Plus” era,” *Jiangnan Forum*, vol. 1, pp. 33–35, May 2016.
- [3] Z. Lei, “The micro-environment study of museum display for Chinese climate adaptability,” *Ph.D. dissertation*, Dept. Arch., Tsinghua Univ., Beijing, China, 2005.
- [4] *CIE 157: Control of Damage to Museum Objects by Optical Radiation*, International Commission on Illumination, 2004.
- [5] *The Standard of Museum Illumination Design (GB/T23863-2009)*, Beijing, China: China Standard Press, 2009.
- [6] J. Wu, “Research of pigments in the pre-Qin and Han dynasties,” *Ph.D. dissertation*, Dept. Arch., Tianjin Univ., Tianjin, China, 2011.
- [7] *TC3-22: Museum Lighting and Protection Against Radiation Damage*, T. I. C. o. m. (ICOM), Division 3 Meeting of CIE, CIE Div. 3, 2003.
- [8] R. L. Feller, “Accelerated aging: Photochemical and thermal aspects,” *Research in Conservation* (Getty Conservation Institute, Marina del Rey, CA), pp. xiv, 275 p, 1994.
- [9] M. Lunz, E. Talgorn, J. Baken, W. Wagemans, and D. Veldman, “Can LEDs help with art conservation?—Impact of different light spectra on paint pigment degradation,” *Stud. Conserv.*, vol. 62, no. 5, pp. 294–303, Jun. 2017.
- [10] R. Sarkar and S. Mazumdar, “Studies and experiments for determination of degradation of paintings in museum art galleries caused by artificial light sources,” *Light Eng.*, vol. 24, no. 2, pp. 12–21, Jan. 2016.
- [11] D. Abdalla, A. Duis, D. Durmus, and W. Davis, “Customisation of light source spectrum to minimise light absorbed by artwork,” in *Proc. CIE Lighting Quality Energy Efficiency*, 2016, pp. 22–31.
- [12] M. Farke, M. Binetti, and O. Hahn, “Light damage to selected organic materials in display cases: A study of different light sources,” *Stud. Conserv.*, vol. 61, no. Sup1, pp. 83–93, Apr. 2016.
- [13] S. M. Pinilla, D. Vazquez, A. A. Fernandez-Balbuena, C. Muro, and J. Munoz, “Spectral damage model for lighted museum paintings: Oil, acrylic and gouache,” *J. Cultural Heritage*, vol. 22, pp. 931–939, Dec. 2016.
- [14] A. Tuzikas, A. Zukauskas, R. Vaicekauskas, A. Petrusis, P. Vitta, and M. Shur, “Artwork visualization using a solid-state lighting engine with controlled photochemical safety,” *Opt. Exp.*, vol. 22, no. 14, pp. 16802–16818, Jun. 2014.
- [15] R. Dang, M. Zhang, G. Liu, J. Yu, and D. Hou, “Investigation and research on display lighting in museum based on protected historical relics,” *C. J. Illumination Eng.*, vol. 24, no. 3, pp. 18–23, Aug. 2013.
- [16] R. Dang, Y. Yuan, C. Luo, and J. Liu, “Chromaticity shifts due to light exposure of inorganic pigments used in traditional Chinese painting,” *Light. Res. Technol.*, vol. 49, no. 7, pp. 818–828, Apr. 2017.
- [17] M. Rea, “Opinion: The future of LED lighting: greater benefit or just lower cost,” *Light. Res. Technol.*, vol. 42, no. 4, pp. 370–370, Dec. 2010.

- [18] D. Vazquez *et al.*, "Point to point multispectral light projection applied to cultural heritage," *Proc. SPIE*, vol. 10379, pp.103790K1–103790K11, Sep. 2017.
- [19] G. He and J. Tang, "Spectral optimization of color temperature tunable white LEDs with excellent color rendering and luminous efficacy," *Opt. Lett.*, vol. 39, no. 19, pp. 5570–5573, Oct. 2014.
- [20] J. H. Oh, S. J. Yang, Y. G. Sung, and Y. R. Do, "Excellent color rendering indexes of multi-package white LEDs," *Opt. Exp.*, vol. 20, no. 18, pp. 20276–20285, Aug. 2012.
- [21] P. Zhong, G. He, and M. Zhang, "Spectral optimization of the color temperature tunable white light-emitting diode (LED) cluster consisting of direct-emission blue and red LEDs and a diphosphor conversion LED," *Opt. Exp.*, vol. 20, no. Sup5, pp. A684–A693, Sep. 2012.
- [22] A. Neumann, J. J. Wierer Jr., W. Davis, Y. Ohno, S. R. Brueck, and J. Y. Tsao, "Four-color laser white illuminant demonstrating high color-rendering quality," *Opt. Exp.*, vol. 19, no. Sup4, pp. A982–A990, Jul. 2011.
- [23] G. X. He and H. F. Yan, "Optimal spectra of the phosphor-coated white LEDs with excellent color rendering property and high luminous efficacy of radiation," *Opt. Exp.*, vol. 19, no. 3, pp. 2519–2529, Jan. 2011.
- [24] D. Y. Lin, P. Zhong, and G. X. He, "Color temperature tunable white LED cluster with color rendering index above 98," *IEEE Photon. Technol. Lett.*, vol. 29, no. 12, pp. 1050–1053, May 2017.
- [25] C. Gomez-Polo, M. Portillo Munoz, M. C. Lorenzo Luengo, P. Vicente, P. Galindo, and A. M. Martin Casado, "Comparison of the CIE Lab and CIE DE2000 color difference formulas," *J. Prosthetic Dentistry*, vol. 115, no. 1, pp. 65–70, Sep. 2016.
- [26] *Code for Design of Museum Building (JGJ 66-2015)*, China Archit. Building Press, Beijing, China, 2015.
- [27] International Commission on Illumination, *A Method for Assessing the Quality of Daylight Simulators for Colorimetry*. Vienna, Austria: Int. Commission Illumination, 1999, pp. 1–10.
- [28] D. L. DiLaura, K. W. Houser, R. G. Mistrick, and G. R. Steffy, *The Lighting Handbook*. New York, NY, USA: Illuminating Eng. Soc., 2011.
- [29] M. Farke, M. Binetti, and O. Hahn, "Light damage to selected organic materials in display cases: A study of different light sources," *Stud. Conserv.*, vol. 61, pp. S83–S93, Apr. 2016.
- [30] J. Liu, C. Mo, and J. Zhang, "Progress of five primary colours LED lighting source technology," *C. J. Illuminating Eng.*, vol. 28, pp. 1–4, Feb. 2017.
- [31] F. Z. Zhang, H. S. Xu, and Z. H. Wang, "Optimizing spectral compositions of multichannel LED light sources by IES colour fidelity index and luminous efficacy of radiation," *Appl. Opt.*, vol. 56, pp. 1962–1971, 2017.
- [32] Y. Ohno, "Spectral design considerations for white LED color rendering," *Opt. Eng.*, vol. 44, no. 11, Nov. 2005, Art. no. 111302.
- [33] G. X. He and L. H. Zheng, "White-light LED clusters with high color rendering," *Opt. Lett.*, vol. 35, no. 17, pp. 2955–2957, Sep. 2010.
- [34] A. C. Robinson and S. D. Quinn, "A brute force method for spatially-enhanced multivariate facet analysis," *Comput. Environ. Urban Syst.*, vol. 67, pp. 28–38, May 2018.
- [35] CIE Publication 13.3, *Method of Measuring and Specifying Colour Rendering of Light Sources*. Vienna, Austria: Int. Commission Illumination, 1995.
- [36] Y. Ohno, "Practical use and calculation of CCT and Duv," *Leukos*, vol. 10, no. 1, pp. 47–55, Oct. 2013.
- [37] C. S. McCamy, "Correlated color temperature as an explicit function of chromaticity coordinates," *Color Res. Appl.*, vol. 17, no. 2, pp. 142–144, Apr. 1992.